中國機械工程學刊第四十六卷第二期第 121~130 頁(民國一百一十四年)
Journal of the Chinese Society of Mechanical Engineers, Vol.46, No.2, pp 121~130 (2025)

Application of Multiclass Classification to Fault Diagnosis in Harmonic Drive

Tsung-Yu Yu*, Nan-Kai Hsieh** and Shiaw-Wu Chen**

Keywords：Harmonic Drive, Prognostic and Health Management (PHM), Machine Learning, Multiclass Classification

ABSTRACT

The harmonic drive has become a critical component in robotic arms, enhancing their load capacity. Therefore, the harmonic drive's health status affects robotic arms' operational stability. This study focused on diagnosing anomalies in harmonic drives before equipment failure. By artificially creating five common types of faults in harmonic drives and collecting vibration signals with a three-axis accelerometer, this study trained and verified the diagnostic capabilities of numerous classification algorithms, namely the random forest, K-Nearest Neighbors (KNN), Support Vector Classification (SVC), and eXtreme Gradient Boosting (XGBoost) algorithms. In the experiments performed in this study, SVC and XGBoost exhibited excellent abilities in identifying harmonic drive faults and classifying potential fault causes. Thus, these algorithms can facilitate the adoption of immediate fault-prevention measures.

INTRODUCTION

In 2022, the usage of industrial robotic arms reached 443,000 units, marking a 22% increase compared to the previous year (Chen et al., 2024). This surge has cemented their role as indispensable equipment in the Aerospace, Precision Medical, and Smart Manufacturing sectors. According to statistics, 40% to 70% of industrial robotic arm failures are attributed to harmonic drives (Bosen et al., 2022). To ensure the stable operation of this critical component and to prevent unexpected failures due to harsh working environments, which could lead to production interruptions and even personnel injuries, there is an urgent need to develop effective health monitoring and fault diagnosis methods. Consequently, improving the operational stability of industrial robotic arms has become a significant focus for researchers in both academia and industry. (Javaid et al., 2021) (Anil Kumar et al., 2022). Conventionally, equipment inspection is conducted by experts with extensive practical threatening to the vehicle occupant. within the experience; however, training such experts is time-consuming, thereby limiting the applicability of this approach. Therefore, machine learning techniques are being increasingly applied for detecting anomalies in equipment, with supervised and unsupervised learning methods being widely used for detecting anomalies in rotating equipment. These methods have achieved superior accuracy in identifying damage, thereby extending equipment life span (Li & Hao, 2022).

In machine learning, supervised and unsupervised learning methods are widely applied for anomaly detection in rotating machinery. Supervised learning requires a large data set with labels, with learning and prediction being performed on the basis of known labels. Unsupervised learning does not require prelabeled data and can discover hidden structures and patterns. With advances in deep learning technologies, methods based on deep learning have shown potential for use in fault diagnoses for rotating machinery (Liu et al., 2018). Deep learning techniques such as convolutional neural networks, recurrent neural networks, and autoencoders are used to process and analyze vibration data from rotating machinery, thereby achieving high fault detection accuracy (Neupane & Seok, 2020). Therefore, sensor data collected through machine learning can be analyzed to predict the health status of equipment and reduce downtime (Yang, Zhong, Yang, Tao, et al., 2021).

Assembly errors and manufacturing defects were identified as the two main causes of harmonic drive failures by previous researchers (Yang, Zhong, Yang, & Du, 2021), which often lead to multiple simultaneous failures in robotic arms (Yang et al., 2023). Researchers (Raviola et al., 2021) identified factors affecting the reliability of robotic arms and harmonic drives; they employed fault tree analyses and

Paper Received April, 2024. Revised August, 2024. Accepted August, 2024. Author for Correspondence: Nan-Kai Hsieh.

* *Ph.D. Program of Electrical and Compunctions Engineering, Feng Chia University, Taiwan, R.O.C.; Department of Computer Science and Information Engineering, National Taichung University of Science and Technology, Taiwan, R.O.C.*

***Department of Automatic Control Engineering, Feng Chia University, Taiwan, R.O.C.*

failure mode, effects, and criticality analyses to identify the causes of component degradation. (Caccavale et al., 2013) and (Mi et al., 2017) installed various sensors at several joints of a robotic arm to collect data on speed, acceleration, and torque to detect early signs of equipment performance decline. The previous investigation (Huan-Kun et al., 2021) identified insufficient lubrication, belt loosening, gear wear, and breakage as common causes of failure in typical robotic arms, and they used principal component analyses and the support vector machine (SVM) algorithm to calculate the robot health index to detect aging and mechanical wear. The present study predicted the health status of harmonic drives by using the K-nearest neighbors (Pan et al., 2020; Pandya et al., 2013), random forest (RF) (Shevchik et al., 2016; Zhou et al., 2013), and SVM (Husari & Seshadrinath, 2021; Li et al., 2018) algorithms to establish a prognostic and health management (PHM) mechanism for subsequent fault diagnoses and maintenance efforts.

Numerous diagnostic methods for rotating machinery failures exist; however, harmonic drive-related fault diagnoses remain an underexplored topic (Yang, Zhong, Yang, & Du, 2021; Yang, Zhong, Yang, Tao, et al., 2021). Building upon the research of Raviola et al. (Raviola et al., 2021), the present study identified five common causes of faults in rotating machinery (Figure 1): (1) gear wear, which can result from shaft eccentricity and excessive shaft surface roughness; (2) gear fracture, which is caused by foreign object entrapment and overload; (3) less grease, which can result from insufficient greasing and grease aging; (4) manufacturing defects, which can be caused by improper or misaligned installation; and (5) improper load, which is the consequence of failure to use equipment according to standard procedures. However, there is still a lack of a systematic diagnostic method for harmonic drives. To address this gap, this paper proposes an effective machine-learning model that leverages a triaxial accelerometer in combination with five fault conditions. The study further investigates the advantages of various analytical methods in fault identification for rotating machinery, with the aim of ensuring the stability of equipment operations.

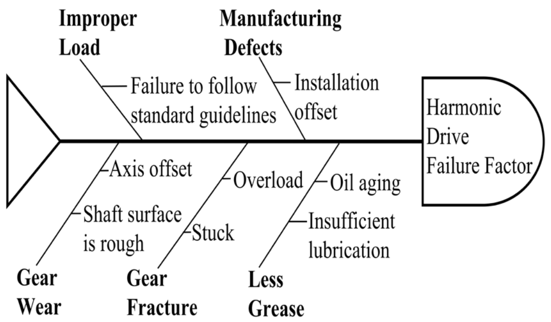

Fig. 1. Analysis chart of common fault causes

The rest of this paper is organized as follows. Method describes four algorithms for multiclass classification, namely K-nearest neighbors, Random forest, eXtreme Gradient Boosting, and support vector classification; Data Preprocessing and Experimental details the data preprocessing and experimental methods used in this study; Experimental Results discusses the classification abilities of the adopted algorithms; and Conclusion provides the conclusion of this study.

LITERATURE REVIEW

Machine learning automatically extract features and perform feature classification and anomaly detection through supervised and unsupervised learning . Supervised learning methods, such as machine learning (ML) and artificial neural networks, rely on labeled datasets for training. In contrast, unsupervised learning methods, such as Principal Component Analysis (PCA) and Independent Component Analysis (ICA), can uncover hidden structures and patterns in unlabeled data, providing the advantage of automatic feature selection.

Among various diagnostic methods, vibration signals have been widely applied in the early fault diagnosis of induction motors. Previous studies have shown that methods such as KNN, SVM, RF, and XGBoost (Chen et al., 2021; Jamil et al., 2021; Shaik et al., 2024) have been extensively used in the fault diagnosis of rotating machinery. KNN is commonly employed in applications like handwritten digit recognition and equipment anomaly classification due to its simplicity and ease of implementation. Similarly, SVM, which uses a statistical learning framework for feature classification, is one of the frequently used ML methods. RF, another common method in ML, allows the definition of feature importance, with the number of labeled samples being a significant factor influencing the classification accuracy of the RF classifier. XGBoost, on the other hand, can handle large datasets and multidimensional features, but careful hyperparameter tuning is required to achieve optimal results in specific problems.

However, most contemporary research on harmonic drives is still focused on deep learning (DL) (Chen et al., 2024; Yang, Zhong, Yang, Tao, et al., 2021). In contrast, ML offers advantages over DL in terms of lower data requirements, shorter training times, and reduced computational resource demands. Therefore, this study proposes an innovative technique that combines raw data with machine learning techniques for the classification of faults in harmonic drives.

METHOD

The KNN, RF, XGBoost, and SVC models were used in this study to validate the applicability of machine learning in anomaly detection for harmonic drives. The machine learning models used in this study for fault detection in rotating machinery are described in the following section.

K-Nearest Neighbors

KNN is a classification algorithm designed for classifying data into known categories. It uses a data set of already classified instances and employs the Euclidean distance to find the KNN to a test sample. The category of the test data is then determined by a majority vote among these neighbors . If $A = (a_1, a_2, \ldots, a_n)$ and $B = (b_1, b_2, \ldots, b_n)$ represent two points in an n-dimensional space, the Euclidean distance between them is defined as follows:

$$\|A - B\| = \sqrt{(a_1 - b_1)^2, (a_2 - b_2)^2, \ldots, (a_n - b_n)^2)} \qquad (1)$$

The decision function of KNN is defined in Equation (2), where A represents the data to be classified, and B_i^c denotes the i th data in the original data set that belongs to class C.

$$Class(D) = min\|A - B_i^c\| \qquad (2)$$

Random Forest

RF is an algorithm used for determining the health status of mechanical equipment. During the training process of this algorithm, the feature set is divided into in-bag (BAG) and out-of-bag (OOB) subsets. For each BAG subset, a decision tree is constructed, and the OOB subset is used to evaluate the decision tree's classification accuracy. The OOB subset from the complete training data set is used to generate the RF algorithm's final outcome, with a majority voting scheme being employed to obtain the final classifier accuracy .

eXtreme Gradient Boosting

XGBoost is an enhanced and optimized version of the Gradient Boosting Machine algorithm. XGBoost is extensively applied in classification applications, and its objective function is expressed as follows:

$$OObjective = \sum_{i=1}^{n} l(y_i, \hat{y}_i) + \sum_{k=1}^{K} \Omega(f_k) \qquad (3)$$

Where $l(y_i,\ \hat{y}_i)$ represents the training loss function and $\sum_{k=1}^{K} \Omega(f_k)$ is the regularization term in the objective function. This term aggregates the complexity of k trees to prevent the model from overfitting.

Support Vector Classification

Similar to SVM, SVC, which is an efficient computational learning method for classifying small data sets, is widely applied in anomaly detection and related fields. The core of the SVC algorithm is its support vectors , which play a crucial role in defining the decision boundaries of the classifier, as illustrated in Figure 2.

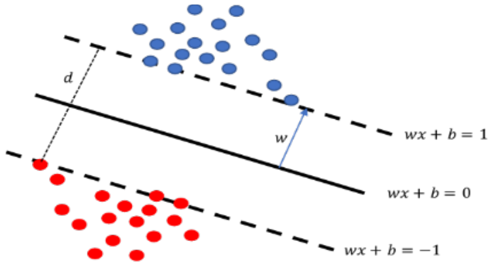

Fig. 2. Decision boundary diagram

Model evaluation

To thoroughly compare the differences between the KNN, RF, XGBoost, and SVC models as model training data sets, this study performed data reduction and K-fold cross-validation for training. In K-fold cross-validation, the original data set is divided into K equal parts. In each training cycle, K − 1 parts are used as the training set, and the remaining part is used as the test set. This process is repeated until each part has served as the test set (Figure 3). In the present study, K was set as 5; thus, five-fold cross-validation was performed (i.e., the data set was divided into five equal parts).

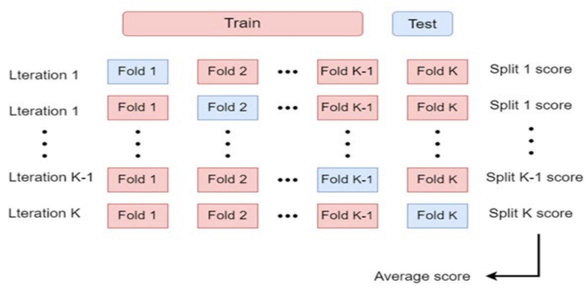

Fig. 3. K-Fold cross-validation diagram

DATA PREPROCESSING AND EXPERIMENTAL

This study established a data set for harmonic drive failures to validate the application of multiclass classification in the diagnoses of faults in rotating machinery. Five fault models were manually created, and triaxial accelerometers were used to collect acceleration signals from these models. Axial measurements for the harmonic drive were conducted along the Z-axis, and radial measurements for the harmonic drive were conducted along the X-axis and Y-axis. We ensured that the three axes were aligned perpendicularly to the axis of rotation to obtain reference points and clear signals (Figure 4). A data acquisition module (ADLink USB-2405) with a sampling rate of 51,200 was used to collect data along the three axes. A total of 170 signal samples with a duration of 1s each were obtained along each axis; thus, 850 signal samples were obtained along each axis across the five fault models for subsequent data analyses.

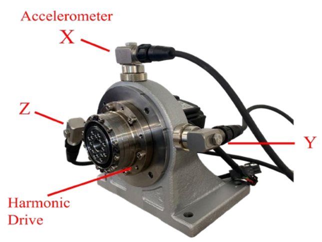

Fig. 4. Harmonic drive signal collection equipment

Original dataset

According to Li and Hao (Li & Hao, 2022) and Raviola et al. (Raviola et al., 2021), the main causes of faults in harmonic drives are equipment aging and improper human operation. Therefore, we distinguished the common states of harmonic drives into five categories, namely normal (N), gear wear (GW), less grease (LG), gear fracture (GF), and improper load (IL), to validate the effectiveness of multiclass classification in predicting harmonic drive faults.

Experimental procedure and equipment

The experiments of this study were performed on a computer with a 12th Gen Intel(R) Core(TM) i5-12500H computer processing unit having a processing speed of 2.50 GHz, an Intel Iris Xe Graphics graphics processing unit, and 16.0 GB of memory. Five fault states were manually established (Table 1), after which signal collection and data preprocessing were performed. Data preprocessing was performed to achieve a processed data format of 170 × 51200, where 170 represents the quantity of single-axis data for a single fault type, and 51200 is the sampling rate for fault identification training. Finally, multiclass classification was performed for accurately classifying the five types of faults, as illustrated in Figure 5.

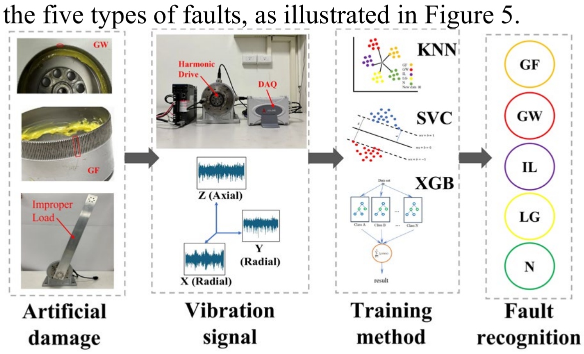

Fig. 5. Experimental flowchart

Table 1. Fault states

Fault Type	Description
Normal (N)	Brand-new equipment is used in this fault model, which serves as a benchmark for comparison against other fault models.
Gear Wear (GW)	The flexspline’s teeth are manually damaged by 50% in this fault model to simulate gear wear.
Gear Fracture (GF)	The distinction between this fault model and the GW model lies in the complete destruction of one of the gears (100% damage) in this model to simulate a gear tooth fracture scenario.
Improper Load (IL)	A 7-kg swing arm is added as an extra load on the harmonic drive in this fault model.
Less Grease (LG)	The use of lubricant is reduced by 90% compared with normal conditions in this fault model.

EXPERIMENTAL RESULTS

We collected vibration signals along the X-axis, Y-axis, and Z-axis of harmonic drives under five fault states. To facilitate model training and validation, the data set was divided into training, testing, and validation sets, which comprised 70%, 20%, and 10% of the data, respectively. The RF, KNN, XGBoost, and SVC algorithms were used for training, and model recognition accuracy was assessed using confusion matrices, F1 score, recall, accuracy, and precision. The classification accuracies of the aforementioned algorithms for the GF, GW, IL, LG, and N fault states are described in the following text.

RF model

As presented in Figure 6~8, when the RF model was used for anomaly detection and classification, the highest prediction accuracies on the X-axis and Y-axis were obtained for the GW fault state, whereas the highest prediction accuracy on the Z-axis was obtained for the IL fault state. Table 2~4 present the evaluation results obtained for the RF model along the X-axis, Y-axis, and Z-axis, respectively.

Table 2. RF classifiers in the X-axis

Fault type	Accuracy	F1-Score	Precision	Recall
GF	0.9045	0.9042	0.9049	0.9078
GW	0.9119	0.9112	0.9116	0.9140
IL	0.9070	0.9062	0.9072	0.9095
LG	0.9053	0.9046	0.9052	0.9079
Normal	0.9069	0.9062	0.9065	0.9107
Average	**0.9071**	0.9065	0.9071	0.9100

Table 3. RF classifiers in the Y-axis

Fault type	Accuracy	F1-Score	Precision	Recall
GF	0.9532	0.9532	0.9534	0.9546
GW	0.9517	0.9517	0.9521	0.9531
IL	0.9521	0.9519	0.9520	0.9535
LG	0.9523	0.9519	0.9520	0.9533
Normal	0.9551	0.9548	0.9547	0.9564
Average	**0.9528**	0.9527	0.9528	0.9542

Table 4. RF classifiers in the Z-axis

Fault type	Accuracy	F1-Score	Precision	Recall
GF	0.8504	0.8485	0.8510	0.8508
GW	0.8549	0.8516	0.8533	0.8551
IL	0.8518	0.8498	0.8526	0.8520
LG	0.8549	0.8524	0.8542	0.8545
Normal	0.8484	0.8467	0.8494	0.8492
Average	**0.8521**	0.8498	0.8521	0.8523

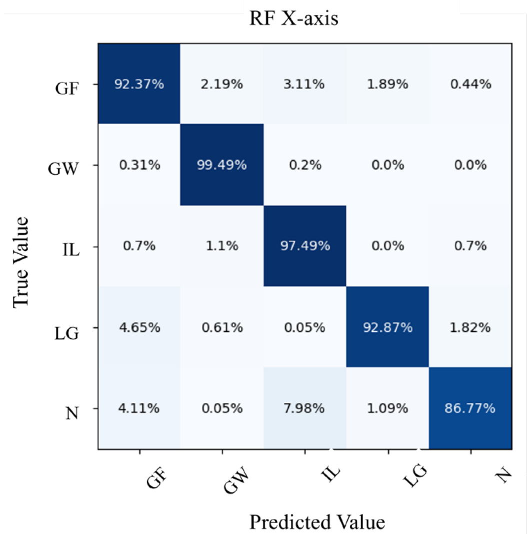

Fig. 6. RF X-axis confusion matrix

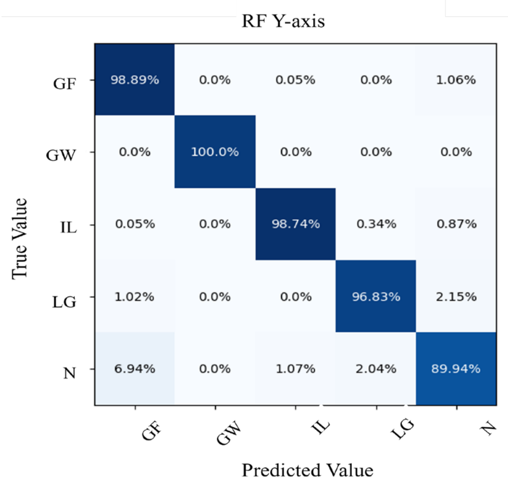

Fig. 7. RF Y-axis confusion matrix

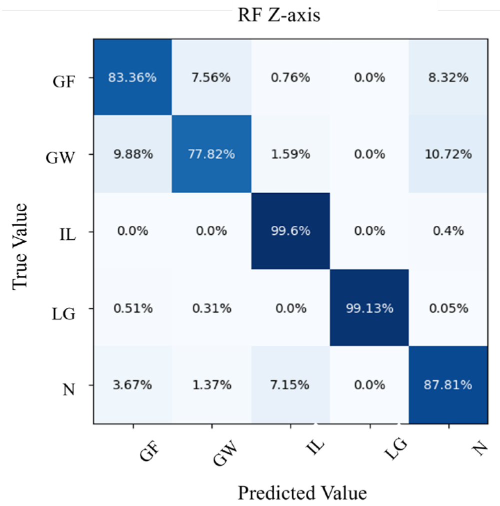

Fig. 8. RF Z-axis confusion matrix

KNN model

As presented in Figure 9~11, when the KNN model was used for anomaly detection and classification, the highest prediction accuracies on the X-axis and Z-axis were obtained for the IL fault state. In contrast, the highest prediction accuracy on the Y-axis was obtained for the GW fault state. Tables 5~7 present the results obtained for the KNN model.

Table 5. KNN classifiers in the X-axis

Fault type	Accuracy	F1-Score	Precision	Recall
GF	0.8062	0.8032	0.8071	0.8411
GW	0.8096	0.8055	0.8093	0.8436
IL	0.8051	0.8008	0.8048	0.8390
LG	0.8103	0.8061	0.8103	0.8429
Normal	0.8063	0.8016	0.8059	0.8392
Average	**0.8075**	0.8034	0.8075	0.8412

Table 6. KNN classifiers in the Y-axis

Fault type	Accuracy	F1-Score	Precision	Recall
GF	0.9543	0.9543	0.9541	0.9573
GW	0.9525	0.9529	0.9527	0.9563
IL	0.9541	0.9540	0.9540	0.9566
LG	0.9542	0.9540	0.9541	0.9567
Normal	0.9538	0.9537	0.9538	0.9564
Average	**0.9537**	0.9538	0.9537	0.9567

Table 7. KNN classifiers in the Z-axis

Fault type	Accuracy	F1-Score	Precision	Recall
GF	0.7708	0.7658	0.7698	0.8092
GW	0.7714	0.7654	0.7709	0.8070
IL	0.7756	0.7714	0.7767	0.8146
LG	0.7775	0.7727	0.7758	0.8132
Normal	0.7690	0.7648	0.7711	0.8085
Average	**0.7728**	0.7680	0.7729	0.8105

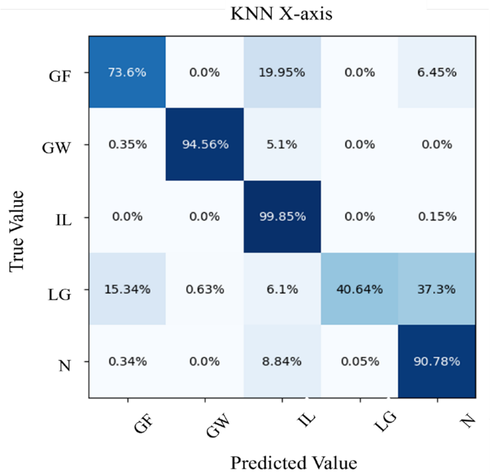

Fig. 9. KNN X-axis confusion matrix

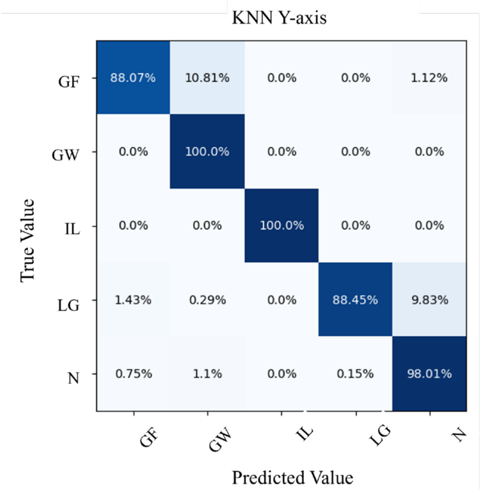

Fig. 10. KNN Y-axis confusion matrix

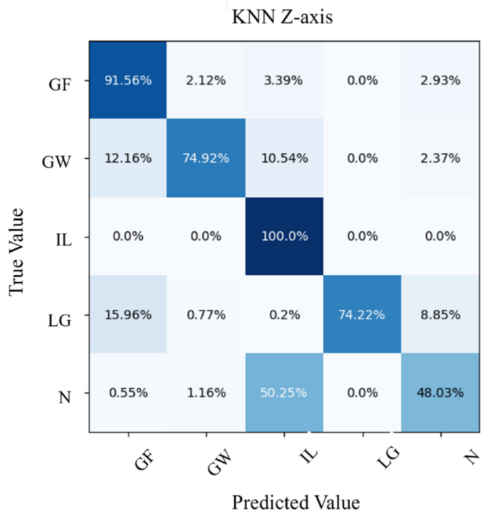

Fig. 11. KNN Z-axis confusion matrix

XGBoost model

As presented in Figure 12~14, when the XGBoost model was used for anomaly detection and classification, the highest prediction accuracies on the X-axis and Y-axis were obtained for the GW fault state, whereas the highest prediction accuracy on the Z-axis was obtained for the IL fault state. Tables 8~10 present the evaluation results obtained for the XGBoost model along the X-axis, Y-axis, and Z-axis, respectively.

Table 8. XGB classifiers in the X-axis

Fault type	Accuracy	F1-Score	Precision	Recall
GF	0.9263	0.9268	0.9270	0.9286
GW	0.9278	0.9281	0.9279	0.9295
IL	0.9302	0.9300	0.9301	0.9313
LG	0.9295	0.9294	0.9293	0.9311
Normal	0.9304	0.9301	0.9299	0.9317
Average	**0.9288**	0.9289	0.9288	0.9304

Table 9. XGB classifiers in the Y-axis

Fault type	Accuracy	F1-Score	Precision	Recall
GF	0.9747	0.9748	0.9748	0.9750
GW	0.9742	0.9744	0.9744	0.9745
IL	0.9744	0.9744	0.9744	0.9747
LG	0.9739	0.9738	0.9737	0.9741
Normal	0.9760	0.9759	0.9758	0.9763
Average	**0.9746**	0.9747	0.9746	0.9749

Table 10. XGB classifiers in the Z-axis

Fault type	Accuracy	F1-Score	Precision	Recall
GF	0.9162	0.9160	0.9164	0.9166
GW	0.9136	0.9126	0.9128	0.9136
IL	0.9128	0.9127	0.9133	0.9134
LG	0.9153	0.9147	0.9148	0.9154
Normal	0.9090	0.9090	0.9096	0.9096
Average	**0.9134**	0.9130	0.9134	0.9137

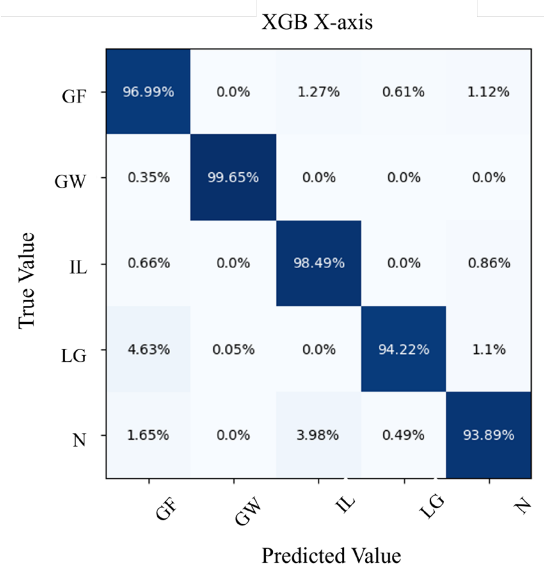

Fig. 12. XGB X-axis confusion matrix

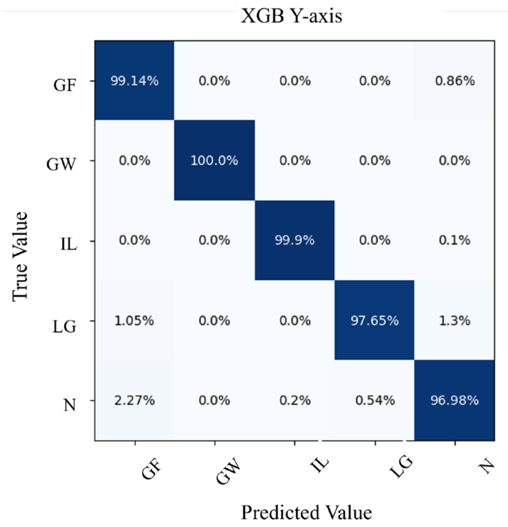

Fig. 13. XGB Y-axis confusion matrix

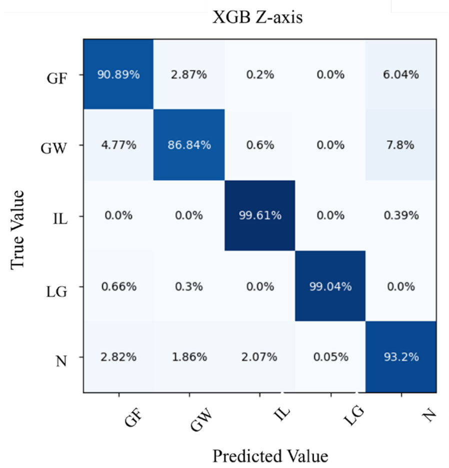

Fig. 14. XGB Z-axis confusion matrix

SVC model

As presented in Figure 14~16, when the SVC model was used for anomaly detection and classification, the highest prediction accuracies on the X-axis and Y-axis were obtained for the GW fault state, whereas the highest prediction accuracy on the *Z*-axis was obtained for the IL fault state. Table 11~13 presents the evaluation results obtained for the SVC model along the X-axis, Y-axis, and Z-axis, respectively.

Table 11. SVC classifiers in the X-axis

Fault type	Accuracy	F1-Score	Precision	Recall
GF	0.9767	0.9767	0.9767	0.9769
GW	0.9774	0.9774	0.9775	0.9776
IL	0.9753	0.9753	0.9753	0.9755
LG	0.9777	0.9776	0.9775	0.9779
Normal	0.9776	0.9775	0.9776	0.9777
Average	**0.9769**	0.9769	0.9769	0.9771

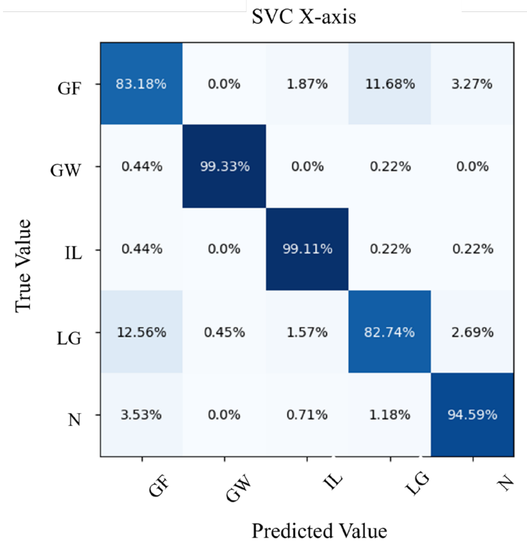

Fig. 14. SVC X-axis confusion matrix

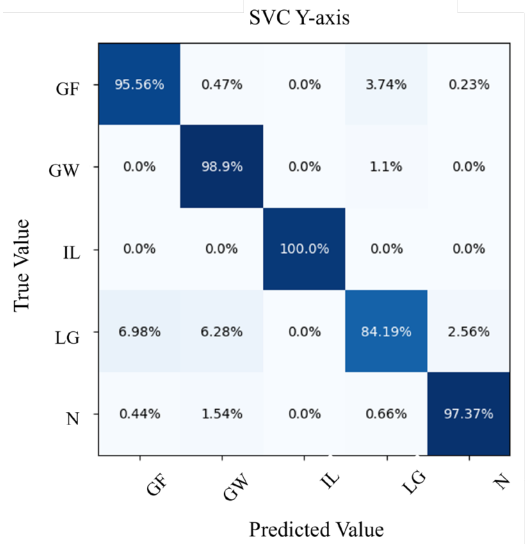

Fig. 15. SVC Y-axis confusion matrix

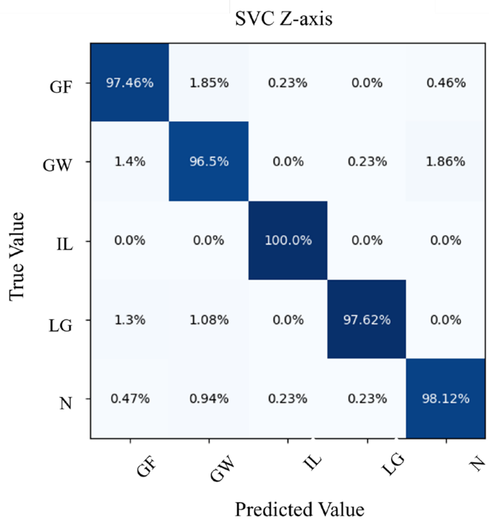

Fig. 16. SVC Z-axis confusion matrix

Table 12. SVC classifiers in the Y-axis

Fault type	Accuracy	F1-Score	Precision	Recall
GF	0.8788	0.8779	0.8789	0.8860
GW	0.8803	0.8785	0.8801	0.8871
IL	0.8793	0.8780	0.8796	0.8867
LG	0.8786	0.8790	0.8842	0.8773
Normal	0.8781	0.8763	0.8775	0.8851
Average	**0.8790**	0.8776	0.8790	0.8858

Table 13. SVC classifiers in the Z-axis

Fault type	Accuracy	F1-Score	Precision	Recall
GF	0.9826	0.9825	0.9825	0.9826
GW	0.9851	0.9851	0.9850	0.9852
IL	0.9824	0.9823	0.9824	0.9824
LG	0.9836	0.9835	0.9835	0.9836
Normal	0.9835	0.9835	0.9835	0.9836
Average	**0.9834**	0.9834	0.9834	0.9835

The vibration of mechanical equipment is typically anisotropic, meaning that the vibration may have different intensities and frequencies in different directions. Accelerometers measure vibration along three distinct axes, which usually correspond to different directions of the mechanical equipment. As a result, the amplitude and frequency of the vibrations captured by each axis can vary, reflecting the characteristics of the vibration in each direction. For the X-axis data, the SVC model achieved the highest accuracy, followed by the XGBoost, RF, and KNN models. Moreover, for the Y-axis data, XGBoost showed the highest accuracy, followed by the KNN, RF, and SVC models. Finally, for the Z-axis data, the SVC model exhibited the highest accuracy, followed by the XGBoost, RF, and KNN models, as shown in Figure 17.

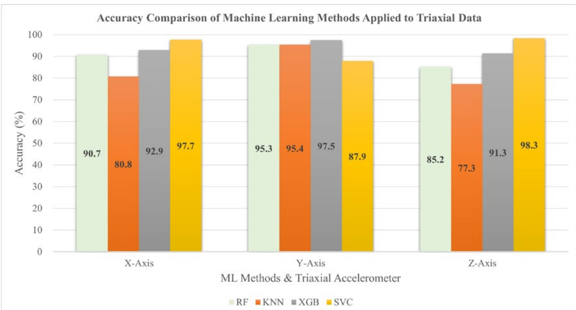

Fig. 17. Accuracy Comparison of Machine Learning Methods Applied to Triaxial Data

These results highlight the superior performance of the SVC and XGBoost models in fault data categorization across various axes. This finding is also supported by the literature, which indicates that SVC is effective in handling high-dimensional data and complex classification (Abdul & Al-Talabani, 2022; Zhang et al., 2022). However, the aforementioned four classifiers exhibited performance variations along the different axes, which underscores the importance of selecting the appropriate classifier according to the data characteristics and classification task.

The results indicate that SVC is the optimal algorithm for predicting the GW fault state on the Z-axis and the LG fault state on the X-axis. In addition, XGBoost is the optimal algorithm for predicting the N fault state on the Y-axis (Table 14). These findings provide crucial insights for enhancing the recognition accuracy of multiclass fault classification models in the monitoring of the operational status of harmonic drives. The results of this study are specific to the adopted data sets and classifiers. Therefore, future studies can examine whether improved outcomes can be achieved using other classifiers or by performing parameter fine-tuning. Moreover, future research can examine whether additional features such as vibration and current signal can further enhance the accuracy and stability of fault prediction models.

Table 14. The best anomaly detection methods and projects for X, Y, and Z axes

Method	X-axis	Y-axis	Z-axis
XGB	-	Normal	-
SVC	Less Grease	-	Gear Wear

CONCLUSION

This study demonstrated the effectiveness and feasibility of using four multiclass classification models, namely the KNN, RF, XGBoost, and SVC models, for predicting the health status of harmonic drives. By enabling the real-time monitoring of the operating conditions of robotic arms, these models facilitate immediate surveillance and maintenance, thereby enhancing production efficiency and reducing downtime. Three-axis vibration data were obtained using accelerometers, and the analyses of these data with the aforementioned models revealed that the SVC model exhibited the optimal performance along the X-axis and Z-axis, whereas the XGBoost exhibited the optimal performance along the Y-axis. These models enable the rapid identification of anomalies in harmonic drives, thereby facilitating efficient PHM.

Overall, the results of this study suggest that multiclass classification is effective for predicting and diagnosing faults in harmonic drives. This method can be used to develop automatic fault prediction and maintenance strategies for industrial manufacturing, thereby facilitating industrial automation. Future studies should continue to investigate the industrial applications of the aforementioned method.

REFERENCES

Abdul, Z. K., & Al-Talabani, A. K. (2022). Highly accurate gear fault diagnosis based on support vector machine. *Journal of Vibration Engineering & Technologies*, 1-13.

Anil Kumar, T. C., Bhusal Sharma, N., Mishra, A. K., Patil, P., Sarveswara Reddy, S., & Bhardwaj, R. (2022). Fault identification model using IIoT for industrial application. *Measurement: Sensors*, *24*, 100526. https://doi.org/https://doi.org/10.1016/j.measen.2022.100526

Bosen, M., Lulu, J., & Jia, W. (2022). Degradation Modeling for the Reducer of Industrial Robot under Periodic Multi-Stage Task. 2022 Global Reliability and Prognostics and Health Management (PHM-Yantai),

Caccavale, F., Marino, A., Muscio, G., & Pierri, F. (2013). Discrete-Time Framework for Fault Diagnosis in Robotic Manipulators. *IEEE Transactions on Control Systems Technology*, *21*(5), 1858-1873. https://doi.org/10.1109/TCST.2012.2212196

Chen, J., Wen, K., Xia, J., Huang, R., Chen, Z., & Li, W. (2024). Knowledge Embedded Autoencoder Network for Harmonic Drive Fault Diagnosis Under Few-Shot Industrial Scenarios. *IEEE Internet of Things Journal*, *11*(13), 22915-22925. https://doi.org/10.1109/JIOT.2024.3362343

Chen, S., Yang, R., & Zhong, M. (2021). Graph-based semi-supervised random forest for rotating machinery gearbox fault diagnosis. *Control Engineering Practice*, *117*, 104952. https://doi.org/https://doi.org/10.1016/j.conengprac.2021.104952

Huan-Kun, H., Hsiang-Yuan, T., Huang, M.-B., & Huang, H.-P. (2021). Intelligent fault detection, diagnosis and health evaluation for industrial robots. *Mechanics*, *27*(1), 70-79.

Husari, F., & Seshadrinath, J. (2021). Incipient interturn fault detection and severity evaluation in electric drive system using hybrid HCNN-SVM based model. *IEEE Transactions on Industrial Informatics*, *18*(3), 1823-1832.

Jamil, M. A., Khan, M. A. A., & Khanam, S. (2021). Feature-based performance of SVM and KNN classifiers for diagnosis of rolling element bearing faults. *Vibroengineering Procedia*, *39*, 36-42.

Javaid, M., Haleem, A., Singh, R. P., Rab, S., & Suman, R. (2021). Upgrading the manufacturing sector via applications of industrial internet of things (IIoT). *Sensors International*, *2*, 100129.

Li, W., & Hao, L. J. (2022). Study on the degradation law of harmonic gear drive backlash with wear and assembly errors. *Engineering Failure Analysis*, *140*, 106614. https://doi.org/https://doi.org/10.1016/j.engfailanal.2022.106614

Li, Y., Liang, X., Wei, Y., & Wang, X. (2018). A method based on refined composite multi-scale symbolic dynamic entropy and ISVM-BT for rotating machinery fault diagnosis. *Neurocomputing*, *315*, 246-260.

Liu, R., Yang, B., Zio, E., & Chen, X. (2018). Artificial intelligence for fault diagnosis of rotating machinery: A review. *Mechanical Systems and Signal Processing*, *108*, 33-47.

Mi, Y., Xu, F., Tan, J., Wang, X., & Liang, B. (2017, 26-28 July 2017). Fault-tolerant control of a 2-DOF robot manipulator using multi-sensor switching strategy. 2017 36th Chinese Control Conference (CCC),

Neupane, D., & Seok, J. (2020). Bearing Fault Detection and Diagnosis Using Case Western Reserve University Dataset With Deep Learning Approaches: A Review. *IEEE Access*, *8*, 93155-93178. https://doi.org/10.1109/ACCESS.2020.2990528

Pan, Y., Pan, Z., Wang, Y., & Wang, W. (2020). A new fast search algorithm for exact k-nearest neighbors based on optimal triangle-inequality-based check strategy. *Knowledge-Based Systems*, *189*, 105088.

Pandya, D., Upadhyay, S. H., & Harsha, S. P. (2013). Fault diagnosis of rolling element bearing with intrinsic mode function of acoustic emission data using APF-KNN. *Expert Systems with Applications*, *40*(10), 4137-4145.

Raviola, A., De Martin, A., Guida, R., Jacazio, G., Mauro, S., & Sorli, M. (2021). Harmonic drive gear failures in industrial robots applications: An overview. PHM Society European Conference,

Shaik, N. B., Jongkittinarukorn, K., & Bingi, K. (2024). XGBoost Based Enhanced Predictive Model for Handling Missing Input Parameters: A Case Study on Gas Turbine. *Case Studies in Chemical and Environmental Engineering*, 100775.

Shevchik, S. A., Saeidi, F., Meylan, B., & Wasmer, K. (2016). Prediction of failure in lubricated surfaces using acoustic time–frequency features and random forest algorithm. *IEEE Transactions on Industrial Informatics*, *13*(4), 1541-1553.

Yang, G., Tao, H., Du, R., & Zhong, Y. (2023). Compound Fault Diagnosis of Harmonic Drives Using Deep Capsule Graph Convolutional Network. *IEEE Transactions on Industrial Electronics*, *70*(4), 4186-4195.

Yang, G., Zhong, Y., Yang, L., & Du, R. (2021). Fault Detection of Harmonic Drive Using Multiscale Convolutional Neural Network. *IEEE Transactions on Instrumentation and*

Measurement, *70*, 1-11. https://doi.org/10.1109/TIM.2020.3024355

Yang, G., Zhong, Y., Yang, L., Tao, H., Li, J., & Du, R. (2021). Fault Diagnosis of Harmonic Drive With Imbalanced Data Using Generative Adversarial Network. *IEEE Transactions on Instrumentation and Measurement*, *70*, 1-11. https://doi.org/10.1109/TIM.2021.3089240

Zhang, J., Zhang, Q., Qin, X., & Sun, Y. (2022). A two-stage fault diagnosis methodology for rotating machinery combining optimized support vector data description and optimized support vector machine. *Measurement*, *200*, 111651.

Zhou, Q., Ning, Y., Zhou, Q., Luo, L., & Lei, J. (2013). Structural damage detection method based on random forests and data fusion. *Structural Health Monitoring*, *12*(1), 48-58.

多類別分類器應用於諧波減速機之故障診斷

游宗育
逢甲大學電機與通訊工程博士學位學程；
國立臺中科技大學資訊工程系

謝男凱　　陳孝武
逢甲大學自動控制工程學系

摘　要

諧波減速機已成為機器手臂中之關鍵零件，並能增強其負載能力。因此，諧波減速機的健康狀態與機器手臂的運行穩定性息息相關。本研究著重於診斷諧波減速機的異常狀況，且以人為方式建立諧波減速機的五種常見故障類型，搭配三顆單軸加速度計收集振動信號。同時，訓練並驗證隨機森林(RF)、K 最近鄰（KNN）、支持向量分類（SVC）和極限梯度提升（XGBoost）等演算法之故障分類能力。最後，藉由實驗證實 SVC 和 XGBoost 在辨識諧波減速機異常和分類潛在故障具較高之準確率。因此，這些演算法將可協助早期故障偵測，且立即採取故障預防措施。